

See discussions, stats, and author profiles for this publication at: <https://www.researchgate.net/publication/231366555>

Experiments in Trickle Beds at the Micro- and Macroscale. Flow Characterization and Onset of Pulsing

ARTICLE *in* INDUSTRIAL & ENGINEERING CHEMISTRY RESEARCH · MAY 1994

Impact Factor: 2.59 · DOI: 10.1021/ie00029a028

CITATIONS

28

READS

30

2 AUTHORS, INCLUDING:



Anastasios J. Karabelas

The Centre for Research and Technology, Hel...

288 PUBLICATIONS 4,416 CITATIONS

SEE PROFILE

Experiments in Trickle Beds at the Micro- and Macroscale. Flow Characterization and Onset of Pulsing

Nikolaos A. Tsochatzidis and Anastasios J. Karabelas*

*Chemical Process Engineering Research Institute and Department of Chemical Engineering,
Aristotle University of Thessaloniki, University Box 455, GR 540 06 Thessaloniki, Greece*

A randomly packed bed of nearly uniform spherical particles is employed to study cocurrent air/water downflow. Using a high-speed video camera, observations are made in the interstices close to the bed wall. Patterns in the microscale (in constrictions and pores), similar to those recently reported for a two-dimensional test section, combine to yield macroscopically observed flow regimes. A gas penetration mechanism is identified as a dominant feature at incipient as well as in well developed pulsing flow. Special attention is paid to pulse formation and growth. A new, nonintrusive conductance technique appears to hold distinct advantages, over other methods, for on-line detecting the onset of the pulsing regime. Time records obtained with this technique complement information from flow visualization, shedding light on the mechanism of transition. Measurements of the trickling/pulsing transition boundary are in fair agreement with other data and model predictions from the literature.

Introduction

The term *trickle beds* is employed here, as usual, to characterize packed beds in which a liquid and a gas flow cocurrently downward. The practical significance of this type of equipment for phase contacting is well-known. Thus, many reviews have appeared in the literature, over the past twenty years, summarizing the state of the art as regards transport phenomena and modeling and design approaches; e.g. Charpentier (1976), Hofmann (1977), Herskowitz and Smith (1983), Dudukovic and Mills (1986), Gianetto and Specchia (1992). Fluid mechanical conditions play a central role in trickle bed reactor operation, directly influencing basic parameters such as pressure drop, liquid holdup, heat and mass transfer, and reaction rates. Consequently, a great deal of effort has been devoted to determining hydrodynamic parameters and their effect on transport processes. The complexity of the problem, however, is such that our level of understanding of the basic processes occurring in the bed interstices is not particularly high (de Santos et al., 1991), and no generally applicable (and reliable) method is available for predicting the hydrodynamic characteristics in trickle beds.

A basic step in a systematic design, or research, effort is to define as best as possible the *flow regime map*. The well-known (e.g. Gianetto et al., 1978) flow regimes in cocurrent downflow of nonfoaming systems through packed beds are as follows:

For the *trickling* regime, observed at relatively small liquid rates and small to moderate gas flow rates, gas-continuous flow prevails in the interstices. In the simpler case of fully wetted particles, the packing surfaces are covered by running continuous liquid films or rivulets.

The *pulsing* regime prevails over a fairly large range of intermediate gas and liquid flow rates. It is characterized macroscopically by the alternating passage of liquid-rich and gas-rich zones.

The *bubbling* regime is identified at relatively high liquid and small gas flow rates. The liquid phase appears to be continuous with the gas dispersed in the form of bubbles.

The *spray* regime is observed at high gas and low liquid rates. The gas phase is reported to be continuous with some entrained droplets.

Techniques employed for identifying the flow patterns commonly include simple visual observations (e.g. Charpentier and Favier, 1975), pressure signals (e.g. Chou et al., 1977; Helwick et al., 1992; Holub et al., 1993), and the use of a movie or a video camera (e.g. Sato et al., 1973; Melli et al., 1990). Kolb et al. (1990) recorded signals of pressure fluctuations and identified acoustic "signatures" of some flow regimes. Latifi et al. (1992) employed a matrix of microelectrodes, mounted flush on the bed wall, in connection with an electrodiffusion technique to identify various flow regimes.

In order to assess the results achievable with various experimental techniques, one should clearly define their *spatial and temporal* resolution characteristics and compare them with typical length and time scales of the processes under investigation. For example, conventional high-speed cinematography can provide very useful information (images) of high spatial and temporal resolution only close to the wall of a transparent bed, but no reliable data can be obtained on the liquid distribution throughout the cross section of a cylindrical bed. Similarly, it is difficult to determine the extent to which a local pressure trace, from a sensitive transducer mounted on the column wall, is representative of conditions far into the bed.

To improve our understanding of the complex processes occurring in trickle beds, we need reliable data at a microscopic length scale to interpret observations and/or data taken at the same time over an appropriate macroscale. That small-scale (or pore-scale) processes can be related to large-scale phenomena, such as pulsing, has been proposed and explored in the literature many years ago (e.g. Sicardi et al., 1979). However, systematically recorded and convincing experimental evidence was presented for the first time only recently by Melli et al. (1990). It was, indeed, demonstrated that flow regimes observed in the macroscale result from a combination of elementary flow patterns prevailing in the microscale. Their study, however, was carried out in a highly idealized experimental setup. Instead of particles they fixed O-rings between parallel transparent walls in order to "mimic the void space of packed beds", facilitating the use of a high-speed video camera. Qualitatively the flow patterns obtained are reported to resemble those found in trickle beds despite the geometrical oversimplifications, the most notable one being the absence of particle-to-particle contact points.

* Author for correspondence. E-mail address: KARABAJ@IASON.CPERI.FORTH.GR.

Obviously, additional similar work with a more realistic geometry is needed.

The work reported here aims at providing new reliable experimental data taken at a micro- and a macroscale in a randomly packed trickle bed. The methods employed include a novel nonintrusive conductance technique for local and cross-sectionally averaged measurements, local pressure traces, and fast video recordings. This work is part of a study on trickle bed fluid mechanics and mass transfer. The particular objective of the present publication is to examine the basic elements of flow regimes at the microscale and to relate them to the patterns observed macroscopically. Furthermore, attention is paid to the onset of pulsing flow—a topic of considerable significance in practice and in modeling.

In the following section the design of experiments is discussed and brief comments are made concerning relevant length and time scales, as well as the possibly prevailing forces in the packing. The experimental techniques are described in the next section, followed by presentation of the results.

Design of Experiments

It was decided to conduct these experiments with uniform glass spheres of 6-mm diameter. This is a realistically small size, often used in similar studies reported in the literature, yet large enough to create an adequate typical pore volume for the following flow visualization and to permit instrumenting individual particles (i.e. to embed sensors, lead wires, etc.). The spheres are unpolished and easily wetted. However, the effect of wettability is not considered in this study. The cylindrical column is made of a 14 cm i.d. transparent Plexiglas tube and has a total length of 124 cm. The column-to-particle diameter ratio, $D/d_p = 23.3$, is deemed quite satisfactory for minimizing wall effects. Recently obtained local mass-transfer data (Tsochatzidis and Karabelas, 1994) suggest that although porosity nonuniformities near the wall may influence quantitatively the flow, they do not affect its qualitative features. The column length is considered sufficient for the (unhindered by end effects) development of pulses and for reliable measurements of pressure drop. Air and water are the fluid phases.

As already stated, two types of length scales can be readily recognized in trickle beds; i.e. a *microscale* associated with the creation of distinct states or patterns of gas/liquid interaction at the pore level and a *macroscale* of magnitude sufficient to accommodate the features of all flow regimes, including pulses. It appears (Melli et al., 1990; de Santos et al., 1991) that the size of a typical constriction in the flow passages could be an appropriate length microscale. Ng (1986) argues that such a representative constriction for uniform spheres is roughly 0.3–0.5 times the particle diameter. Also Saez and Carbonell (1985) propose a characteristic length defined as

$$d_p \epsilon / (1 - \epsilon)$$

where ϵ is the bed porosity. This quantity is close to the particle radius. Thus, for simplicity we select here as a microscale the particle radius, r_p . As the macroscale in this system one can choose the bed radius, R , since integration over this length can provide a representative cross-sectional average for most of the main parameters, such as mean porosity, transport coefficients, liquid holdup, and reaction rate. It can also be shown (e.g. using data of Blok and Drinkenburg, 1982) that in the present

system a dynamic length scale, the length of the liquid-rich portion of a pulse, is coincidentally of the same order of magnitude as R . However, this coincidental relationship may not apply in much larger diameter beds.

It is quite important for designing experiments and for properly interpreting data to define *time scales* as well. The ratio of a typical pore size (usually taken equal to particle diameter) over the real gas or liquid velocity (u_g or u_l) provides representative time microscales (d_p/u_g or d_p/u_l , respectively) for gas-continuous or liquid-continuous situations. This ratio is a measure of the residence time of each fluid in a typical "pore", also referred to as "site" by Melli et al. (1990). In our system, the order of magnitude of this microscale is estimated to be between 10^{-3} and 10^{-2} s. A representative value for gas-continuous interstitial conditions is 0.01 s. With regard to a time macroscale one may turn to the pulsing flow regime to identify a relevant quantity. The mean period between pulses appears to be an appropriate time macroscale, representing the largest flow disturbances in the system. Using pulse frequency data (Tsochatzidis and Karabelas, 1991; Block and Drinkenburg, 1982) one observes that the order of magnitude of this time scale remains on the order of 1 s over a large range of flow rates, despite a tendency to decrease with increasing gas and liquid velocities. It is noted that Helwick et al. (1992), on the basis of pressure measurements, suggest that the period between pulses scales with a modified Reynolds number.

To evaluate the relative significance of inertial, viscous, capillary, and gravitational forces considered to play a role in these gas/liquid systems, one usually resorts to the following dimensionless numbers: the Reynolds number of each phase (ratio of inertial and viscous forces), the capillary number (ratio between viscous and capillary forces), the Bond number (ratio between gravitational and capillary forces), and the viscosity and density ratios. de Santos et al. (1991) provide useful comments on such dimensionless numbers for two-phase flow in fine porous media, packed beds, and tubes. The following ranges of these numbers represent conditions covered in this study, by using the particle radius as the characteristic length scale and the real velocities of each phase for reasons previously outlined. σ is the surface tension and g is the

$Re_g = \rho_g u_g r_p / \mu_g$	~50–450
$Re_l = \rho_l u_l r_p / \mu_l$	~150–600
$Ca_l = \mu_l u_l / \sigma$	$\sim 5 \times 10^{-4}$ to 3×10^{-3}
$Bo = r_p^2 (\rho_l - \rho_g) g / \sigma$	~1.2
μ_g / μ_l	$\sim 1.8 \times 10^{-2}$
ρ_g / ρ_l	$\sim 1 \times 10^{-3}$

acceleration due to gravity. It is clear that inertial, capillary, and gravitational forces are quite significant. Even viscous forces, however, which appear to be comparatively less influential in our system, cannot be ignored in general. The significance of capillarity forces [$Bo = O(1)$] is obvious.

Experimental Setup and Procedures

A schematic of the experimental system is shown in Figure 1. The flow rates of air and water are measured by means of calibrated rotameters. Dry filtered air is saturated with water before entering the column, to avoid temperature gradients due to evaporation. To minimize air flow fluctuations, a dampener is used. The experimental runs are carried out at room temperature (about 20 °C). Water is collected in a tank and recirculated, its temperature being practically constant during the tests. Water is sprayed uniformly onto the top of the packing

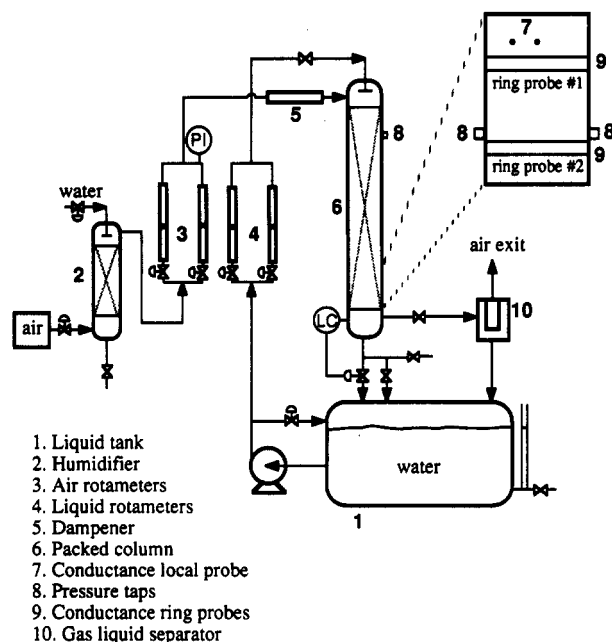


Figure 1. Schematic of experimental setup.

through a perforated disk distributor having approximately 80 small holes. Air is introduced by means of another perforated tube of circular shape, placed at the circumference of the liquid distributor.

The particles are fairly uniform unpolished glass spheres of 6-mm diameter. The column is packed layer by layer to make sure that the porosity of the bed is uniform. The void fraction of the bed was determined to be 0.36. The packing material is supported, at the bottom of the column, by a stainless steel screen.

A newly developed conductance technique is employed which is capable of providing accurate instantaneous holdup measurements in the macroscale. Two identical conductance probes were installed in the lower half of the packed column. Each probe consisted of two ring electrodes flush mounted onto the column wall to avoid disturbing the local porosity of the bed. The performance of these probes measuring conductance of gas/liquid mixtures in pipes and packed beds has been studied experimentally and theoretically by Tsouhatzidis et al. (1992). The same type of electrodes have already been used in studies of two-phase flow in pipes (Andreussi et al., 1988). The ring electrodes have a width of 3 mm. A distance of 3 cm between the electrodes is chosen in order to achieve satisfactory spatial resolution with respect to the length macroscale. Hence, the ring spacing is shorter than the length of the disturbances (pulses) to be investigated. Other criteria for selecting the above ring electrode spacing are discussed by Tsouhatzidis et al. (1992). In the same paper it is shown that the distance of 7 cm of the lower ring electrode from the bottom of the bed is more than adequate to avoid end effects.

An ac carrier voltage of 25-kHz frequency is applied across each probe in order to eliminate capacitive impedance. Selection of the appropriate ac frequency value is made by measuring impedance magnitude and phase of the probe response under various frequencies. An electronic signal analyzer converts the response to an analog output signal (Tsouhatzidis et al., 1992). The analyzers are characterized by high sensitivity and stability. The analog signal from the probes is uniquely related to the conductance (or the liquid holdup) of the medium between the electrodes. Each probe is connected to a separate analyzer to permit simultaneous measurements. Testing

and adjustment of each analyzer is necessary before each set of measurements by using precision resistors.

The analog signals from the analyzers are fed to an A/D converter and recorded in a computer. A sampling rate of 100 Hz is sufficient, and data are collected over a time period of 20.48 s, much larger than the time macroscale.

To further examine liquid holdup characteristics, a separate *local* conductance probe is employed. This probe consists of a pair of metal spheres having dimensions the same as those of the packing material. The first sphere is placed at the center of the bed cross section and 4.5 cm above the upper ring probe while the second is placed at the same level and at a radial distance of 3.5 cm (half the bed radius) from the first sphere (see Figure 1). This arrangement of the local probe can give useful information about conditions in the central part of the bed cross section. Lead wires are accommodated by drilling holes through neighboring particles so that the local voidage is unaffected. The same electronic setup employed for the conductance ring probe is used with the local probe.

For the measurement of two-phase pressure drop through the bed and the recording of pressure fluctuations due to pulses, pressure taps were drilled in the column wall and sensitive pressure transducers (R.D.P. Electronics Ltd., Model TJE true gauge) were flush mounted. The attachments for mounting the transducers were inclined and designed so as to provide the capability of gas purging. In that way the short passage between inner column wall and pressure sensor was always filled with liquid to avoid damping of pressure fluctuations. A transducer was placed at the lower half of the column (Figure 1). It could detect pressures in the range 0–5 psig, with an accuracy of $\pm 0.1\%$ F.S. (full scale) and frequency response of 1 kHz. The output signal of the transducer was fed to an A/D converter and stored in a computer, with a sampling frequency of 100 Hz, to obtain time records of local pressure.

Visual Observations

Flow visualizations of sufficient spatial and temporal resolution (that is at the microscale) are reported here. Their scope is to systematically record flow conditions, to confirm or restate direct observations and speculations made in the literature, and to extract information necessary for the interpretation of the other (local and average) types of data obtained under the same conditions.

Images of the flow are recorded by using a color high-speed video camera (NAC, Model HVS-400). Speeds of 200 and 400 frames/s are used to videotape the bed. The camera focuses at the lower end of the transparent column (approximately 30 cm from the bottom of the bed) at the height where the upper conductance ring probe is placed, to insure that flow conditions are well developed. Two lenses are used depending upon the area of the column observed. With the first lens almost all the cross section of the bed, with a height of about 10 cm, is viewed for flow visualization of the macroscale. The second lens offers the possibility of focusing into the pores near the wall in order to gain qualitative understanding of the flow conditions in the microscale. Representative frames of all the flow regimes observed in trickle beds are recorded to be examined later. The column was always operated first under conditions of high liquid flow rates, in pulsing flow, to ensure complete wetting of the packing, before the flow rates were set at the desired values. Only the more informative photographs taken at the microscale are presented for the following discussion. Observations from the videorecordings in the macroscale are also summarized. The chart in Figure 2 shows the flow rates at which

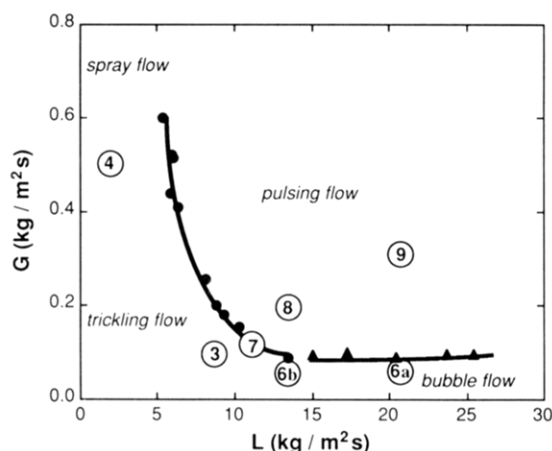


Figure 2. Flow map indicating conditions at which photographs were taken. Numbers in circles correspond to following figure numbers.

photographs (presented here) were taken. The numbers identify conditions of subsequently presented figures.

Elemental Flow Patterns. It is widely accepted in the literature and confirmed in this study that the two major geometrical components of the packing interstices are the larger "pores" or "sites" and the smaller "passages" or "constrictions". Observations concerning pores and passages similar to those reported by Melli et al. (1990) for the two-dimensional bed have been made close to the wall of our column. For the sake of brevity, repeated reference will be made here to their work, where the flow patterns in the microscale are well documented.

Regarding the microscale flow in the *constrictions*, our observations confirm the elemental patterns identified by Melli et al. (1990) with one exception, i.e. that of the *spray* regime. As can be seen in following figures, the patterns referred to as *gas-continuous, bridged, flooded, bubbling, and dispersed bubbling* are present in the three-dimensional beds as well. The inability to discern the spray regime in the present tests may be due to restrictions placed on the maximum gas flow rate. It will be added that in this bed the much more irregular cross sections of constrictions (compared to the square cross sections of Melli et al., 1990) make observations and pattern identification more difficult.

The characterization of flow patterns in the pores can be made on the basis of *gas dominated, liquid dominated, and contested sites*. The latter term appears to cover, in random packed beds, not just one situation but a variety of complex patterns.

Gas- and Liquid-Continuous Macroscale Patterns. The *trickling* flow regime (Figure 3) is essentially gas-continuous. In this and in subsequent pictures, the first number designates the sequence and the other three designate the time (min, s, ms). In the trickling regime the liquid moves downward mainly through rivulets or larger "filaments", as Lutran et al. (1991) observe. There are relatively large areas of the packing with apparently no contribution to the liquid flow. Only stagnant liquid is observed in these areas, trapped from the previous operation of the column at high flow rates. Liquid in these regions moves downward through transient connections of the stagnant liquid zones among the packing particles or between the particles and the wall. Pendant drops sometimes hang from particles and drip to neighboring ones. In this way small quantities of liquid are transferred from regions outside the filaments. The same phenomenon is more pronounced in the spray flow regime.

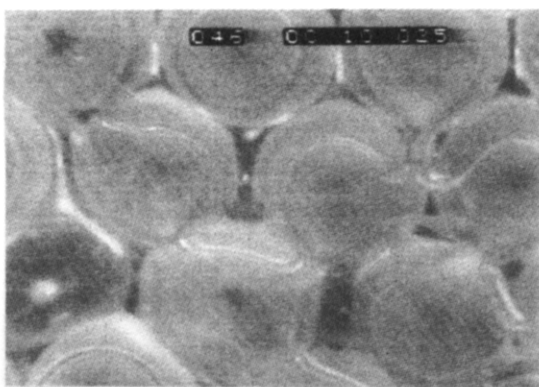


Figure 3. Part of the packing with a filament in the trickling flow regime: $L = 9.243 \text{ kg/m}^2 \text{ s}$ and $G = 0.097 \text{ kg/m}^2 \text{ s}$.

The photograph in Figure 3 shows part of the packing with a liquid filament. It is observed that filaments are very active. Usually they change flow directions while moving downward and their boundaries wet the particles in a wavy mode by frequent modification of their shape, possibly due to the action of capillary forces. Sometimes filaments carry downstream small bubbles (from particle to particle), but this is not a usual occurrence, since air has enough free space to flow. As the liquid flow rate is increased, the number and the thickness of the filaments is also increased. An increase of the gas flow rate tends to increase the number and especially the activity of the filaments (liquid velocity, changing directions, carrying of bubbles). As the flow rates get close to the trickling-to-pulsing flow transition, many filaments become thick and give the impression of "protapses" (small liquid-rich clusters, reported by Melli et al., 1990), which are discussed in the following section. With regard to the elemental flow patterns in the constrictions, one can readily observe gas-continuous, liquid bridged, and flooded passages.

At low liquid and high gas flow rates the *spray flow* regime is obtained, in which filaments no longer exist. Liquid is also transferred in this region through transient connections of the stagnant liquid zones. The gas flow apparently supplies the force required for this liquid movement. There are some preferable passages, like rivulets, but the flow there appears macroscopically discontinuous. Photographs in Figure 4 show a mode of liquid transfer in this flow regime. A pendant drop develops; then a bridge is formed with apparently stagnant liquid at a neighboring particle, and the resulting larger liquid mass moves downstream, possibly through the action of gravity. The time period between the first and the second picture is 10 ms. Melli et al. (1990) report that in the spray flow regime drops are torn off from the trembling liquid suspended from the particles and carried away in the continuous gas flow. This is very likely to happen in beds of large porosity where large empty sites exist between the particles. However, in our column with relatively low void fraction and with several contact points on each particle, isolated drops were not observed. It is possible, however, that at much higher gas flow rates, than those indicated in Figure 4, some short-lived drops may be generated.

It is noted that the Bond number of our system is on the order of 1, so that gravitational and surface forces are comparable, permitting the development of pendant drops. Gas/liquid interface forces, due to high gas velocity, are also considered important for dragging liquid downward. The trickling-to-spray flow transition is very gradual, as these regimes are similar and gas-continuous. The sig-

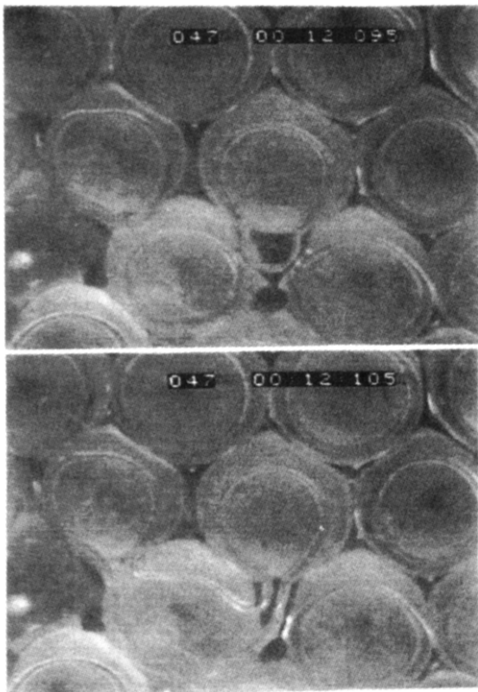


Figure 4. Mode of liquid transfer in the spray flow regime. The flow rates are $L = 2.426 \text{ kg/m}^2 \text{ s}$ and $G = 0.485 \text{ kg/m}^2 \text{ s}$.

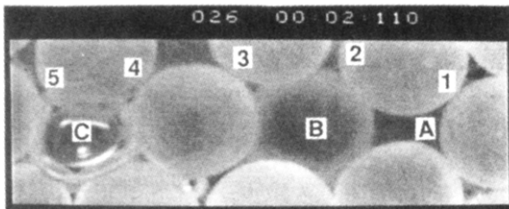


Figure 5. Constricted passages (1–5) and pores or sites (A–C) near the wall of the packed bed. Pore C is occupied by a large bubble.

nificant difference is that “filaments” do not exist in developed “spray” flow, leading to a liquid-discontinuous regime in the macroscale. It is perhaps for this reason that Sato et al. (1973) group the “channeled” and “blurring” flows (as they call the trickling and spray regimes) in the same category of gas-continuous flows.

To facilitate the discussion of the following flow patterns (especially that of pulsing flow), we concentrate on a region of the packed bed near the cylindrical wall, as shown in Figure 5 for a liquid filled bed. Two large pores (B and C) are easily identified as well as a small one (A). The constricted passages (1–5) feed these sites; e.g., passages 2 and 3 feed pore B, while 4 and 5 are connected to pore C.

At high liquid and low gas flow rates, *bubble flow* is observed. This is a liquid-continuous regime, as shown in Figure 6a. Gas flows in a discontinuous mode in a form of fairly large bubbles of various shapes. With increasing gas flow rate, the number and the volume of the bubbles tends to increase. Figure 6a shows that (at those flow rates) relatively large bubbles tend to pass through the constrictions, deforming in the process. At higher gas and liquid flow rates, a case which is occasionally referred to in the literature as the *dispersed bubble regime*, very big gas bubbles were observed, sometimes spanning more than one pore of the bed. The elemental flow patterns which are readily observed at the constrictions (in macroscopically bubble flow) are the bridged, flooded, and bubbling modes.

The transition from trickling to bubbling regime appears to be again gradual. With increasing liquid flow rate, the

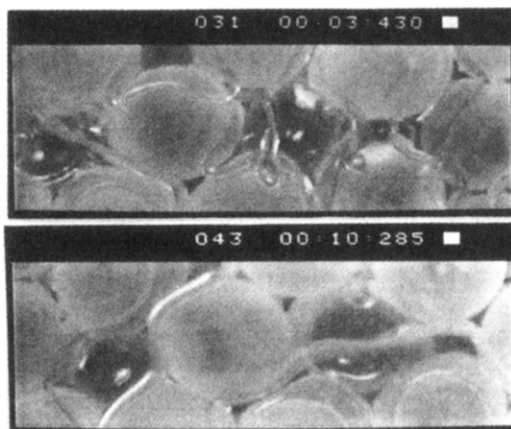


Figure 6. (a, top) Bubble flow regime in the microscale: $L = 20.51 \text{ kg/m}^2 \text{ s}$ and $G = 0.073 \text{ kg/m}^2 \text{ s}$. (b, bottom) Trickling to bubble transition in the microscale: $L = 13.43 \text{ kg/m}^2 \text{ s}$ and $G = 0.055 \text{ kg/m}^2 \text{ s}$.

passages are extensively flooded, creating large liquid-continuous regions, while gas is at the same time a continuous phase. This is clearly shown in the picture of Figure 6b taken at the trickling-to-bubble transition. Passage 4 and pore C operate in a gas-continuous mode, while the neighboring passages 1–3 are flooded. Pore B is half liquid filled.

Pulsing Flow Regime. Macroscopically this regime appears to be a succession of zones; i.e. of moving bubble flow (the liquid-rich zone of a pulse) and of trickling flow (the gas-rich zone). In the latter, rivulets are observed, much like in the trickling regime, while in the former the bubble activity seems to be greater than that in the regular bubble flow pattern.

The sequence of pictures shown in Figure 7 is very helpful to understand the mechanism of trickling-to-pulsing transition and to demonstrate an important feature of the pulsing flow itself. This sequence, as marked in the time indicator, represents events lasting only 12.5 ms. The conditions are those of trickling flow just below (or at) the transition boundary to pulsing flow. Broad liquid filaments connect neighboring particles, while the main flow is gas-continuous, as expected to occur in trickling flow. At (relative) time 440 ms the pores A–C are totally gas dominated, while essentially all the passages (1–5 in Figure 7) appear to be “bridged” (liquid blocked). At time 445 ms, activity is evident at the largest passage (2), through which a bubble is developing. Rapidly the bubble grows to cover the entire pore B, collapsing thereafter when it can no longer be accommodated in the available space. It is important that this bubble grows within a *liquid-empty* pore; that is, the liquid in the passage is adequate and/or surface tension forces are strong enough to allow the creation of this extra gas/liquid interfacial area.

The above bubble formation indicates that the system is close to pulsing flow. Indeed, the simultaneous occlusion (bridging) of several neighboring passages unavoidably leads to pressure gradients which, as will be further discussed, can drive downward liquid-rich pulses. It will be pointed out that this process of gas penetration through the pores (or sites) and the associated very rapid creation and destruction (essentially renewal) of gas/liquid interfacial area have not been reported in the relevant literature so far. This mode of gas penetration appears to be characteristic of the entire pulsing flow regime, as shown in following pictures.

The sequence of pictures in Figure 8 represents flow rates well within the pulsing regime although under these

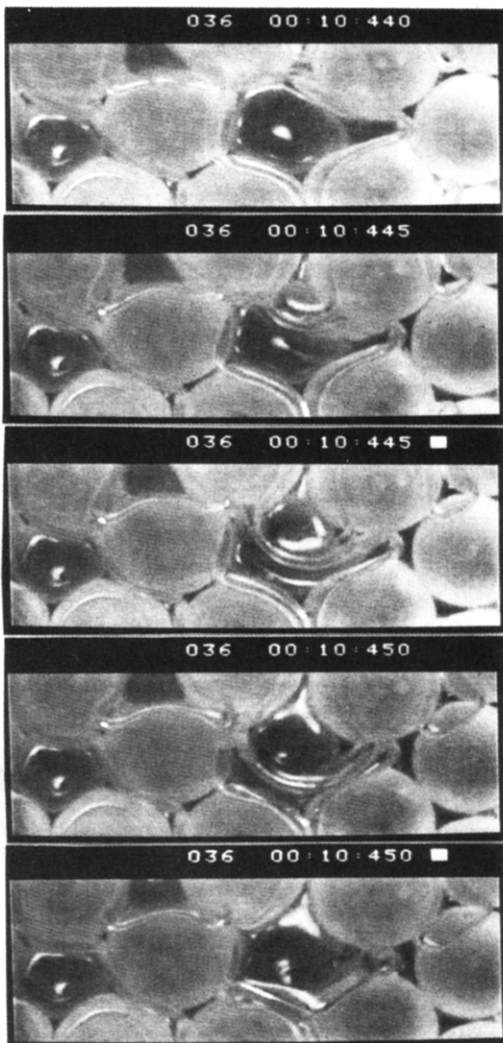


Figure 7. Mode of gas penetration into pores at the trickling-to-pulsing transition boundary. Bubble developing into pore B: $L = 10.85 \text{ kg/m}^2 \text{ s}$ and $G = 0.121 \text{ kg/m}^2 \text{ s}$.

conditions it is considered to be "mild pulsing" flow. At time 115+ ms (actually 117.5 ms) the observed region operates in the gas-rich zone, as evidenced by the isolated liquid areas around contact points. Most of the passages (1, 3, and 4) are open while passage 2 is blocked. At time 120 ms there is evidence of the fast approaching liquid-rich zone; a bubble develops through passage 2, while constrictions 3 and 4 are bridged. Five milliseconds later (time 125 ms) gas is forced through passages 3 and 4. It is noteworthy that two bubbles appear to develop simultaneously (into site B) through constrictions 2 and 3. These bubbles seem to be separated by a thin, nearly vertical, liquid film, dividing site B into two parts, as shown also in the picture for 125+ ms.

Some instances of the evolution of a pulse, as identified by microscale flow modifications, are presented in Figure 9 for relatively high gas and liquid rates; i.e. far into the pulsing regime. At time 585 ms the observed region operates in the gas-rich zone with all the passages open (gas-continuous). At 585+ ms the approach of the liquid-rich zone is clear; i.e., all the constricted passages tend to be bridged. At time 590 ms bubbles are developing through passages 2 and 4, into sites B and C, respectively. At 590+ ms bubbles are created through *all* the observed passages (1–4) into the pores A–C. The increase of the liquid holdup is evident. The sequence of three pictures (585+ through 590+ ms) represents the front of the liquid-rich zone.

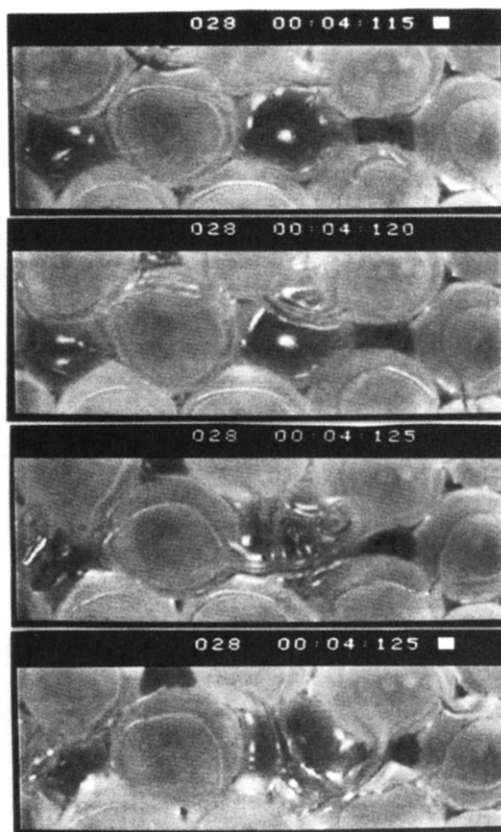


Figure 8. "Mild pulsing" in the microscale. Sequence of pictures at the front of liquid-rich zone: $L = 13.43 \text{ kg/m}^2 \text{ s}$ and $G = 0.195 \text{ kg/m}^2 \text{ s}$.

Somewhat later (time 610 ms) the bubble generation activity is still taking place and all the sites are definitely "contested" in the Melli et al. (1990) terminology. At time 625 ms small bubbles exist, but at the same time, some pores (B and C) are gas-dominated and others (A) appear to be liquid-dominated. Later (pictures at times 705+ and 725 ms) the area of observations is gradually occupied by the gas-rich part of the pulse. First, the bubbles are drastically reduced in number, rivulets are forming connecting neighboring particles, and the (previously highly agitated) gas/liquid interfaces become smooth, as in trickling flow.

Some additional observations concerning pulsing at the microscale are in order. There appears to be no time during the liquid-rich zone that pores on a cross section were 100% liquid-dominated. In fact, no totally liquid-filled relatively large pore was observed in that zone during the tests. This is apparently due to the intensive bubble generation and penetration through the constrictions into the pores. It is possible, however, that very small pores are filled temporarily 100% with liquid. On the other hand, practically all the kinds of microscale flow patterns reported by Melli et al. (1990) are also noted in the constricted passages of the 3-D bed. The lifetime of bubbles developing into the observed large pores is estimated to be about 10 ms, getting shorter for the smaller pores. Melli et al. (1990) report that the filling-emptying cyclic sequence in the microscale of their setup is on the order of 1 ms or less, even though they made observations in relatively large pores.

A few observations in the macroscale are worth reporting. In general, the pulses appear to be axisymmetric with their front on a horizontal plane. Occasionally, however, and only close to the trickling transition region, the front of pulses seems to move at a slight inclination with respect

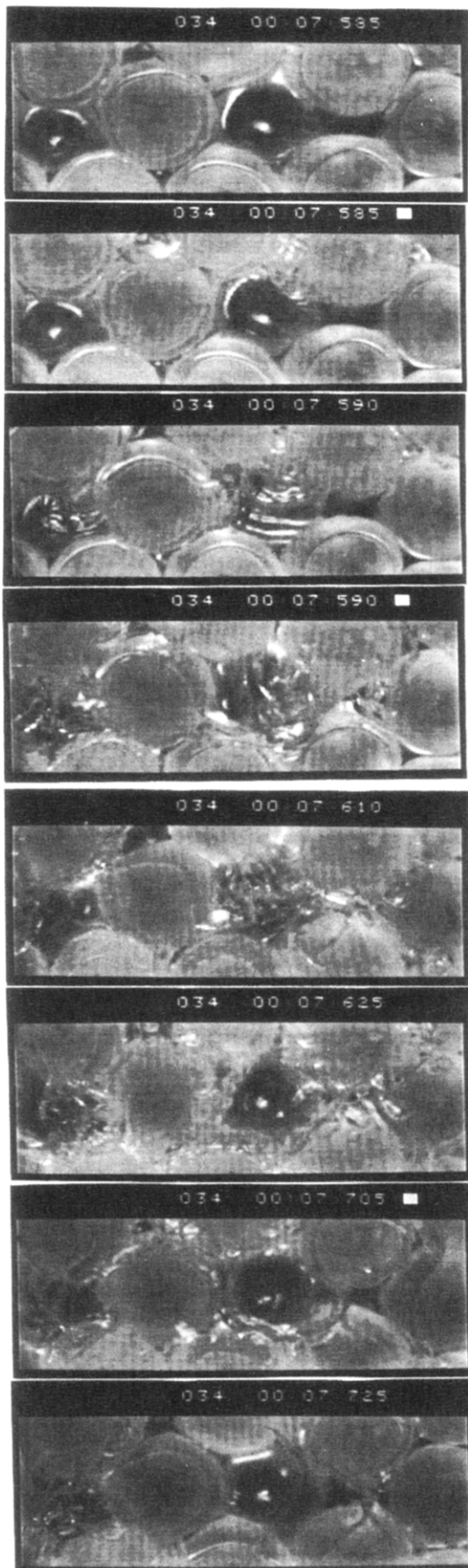


Figure 9. Typical instances of pulse downflow in well developed pulsing flow: $L = 20.51 \text{ kg/m}^2 \text{ s}$ and $G = 0.257 \text{ kg/m}^2 \text{ s}$.

to the horizontal plane. This inclination (right or left) is not systematic, suggesting that it is a dynamic effect during pulse development, rather than the result of geometric bed (porosity) imperfections. Macroscopic determination

of pulse length characteristics is not easy. The liquid-rich zone of a pulse is characterized by a very sharp front (easily detectable, e.g. the photograph for 585+ ms in Figure 9) followed by a gradual decrease of the holdup at its back with no clear boundaries. At flow conditions of mild pulsing not far from the transition region, the liquid-rich zone length is estimated to be 3–5 cm (from the video recordings). At higher flow rates this length can increase by about 2–3 times, or even more in some cases.

Onset of Pulsing Flow

Assessment of Techniques. Particular attention is given here to the important case of trickling-to-pulsing transition. The respective transition boundary is quite extensive, covering flow rates of industrial significance. Most of the literature data on the transition-to-pulsing flow rely on direct visual observations of the first occurrence of a pulse (e.g. Charpentier and Favier, 1975). Holub et al. (1993) determine transition by observing the cessation of pressure fluctuations when reducing flow rates from pulsing to trickling flow and by visual inspection. Other indirect instrumental methods involve sensors mounted on the bed wall. Chou et al. (1977) determined the transition boundary as the condition at which a slight increase in gas or liquid rate caused a sharp increase of the root mean square of wall pressure fluctuations. Latifi et al. (1992) used a matrix of microelectrodes on the bed wall to determine flow regimes by analyzing the fluctuating signals. This off-line technique gave results similar to visual observations.

The nonintrusive conductance technique employed in this study has definite advantages over other methods of the literature in that it permits an *on-line* determination of the transition boundary with very good sensitivity. Preliminary data obtained with the dual-ring probes have already been reported in a conference (Tsochatzidis and Karabelas, 1991). To briefly assess the performance of this technique, with reference to other instrumental methods at our disposal (for detecting transition and measuring pulsing flow properties), comparisons follow between data from the dual-ring probes, the "local" probe, and the sensitive pressure transducer.

Pulses always appear first at the bottom of the bed where the gas velocity is higher due to lower pressure and to gas expansion, as reported in the literature (e.g. Ng, 1986). Therefore, our systematic observations are focused on that section. Two ring probes are employed, placed 20 cm apart (Figure 1). The so-called local conductance probe is located 4.5 cm above the upper ring probe, and the pressure transducer 3.5 cm above the level of the lower ring probe. Figure 10 includes traces taken under the same conditions, slightly above the transition boundary, in pulsing flow. Figure 10a shows simultaneously recorded traces with the two versions of the conductance technique. The response of these probes is very similar, and the pulses (under development) are generally well represented in both traces. The local probe, being influenced by conditions over a much smaller area, compared to the ring probe, displays a much broader spectrum of frequencies of holdup fluctuations. However, this is not an advantage for the present applications, since local packing voidage or flow nonuniformities may contribute to these relatively high and intermediate frequency fluctuations, producing a somewhat confused picture. On the contrary, the ring probe provides a more satisfactory representation of conditions in the macroscale, with sharper definition of pulses. Nevertheless, the clear identification of pulses by both "local" and "ring" probes suggests that conditions in

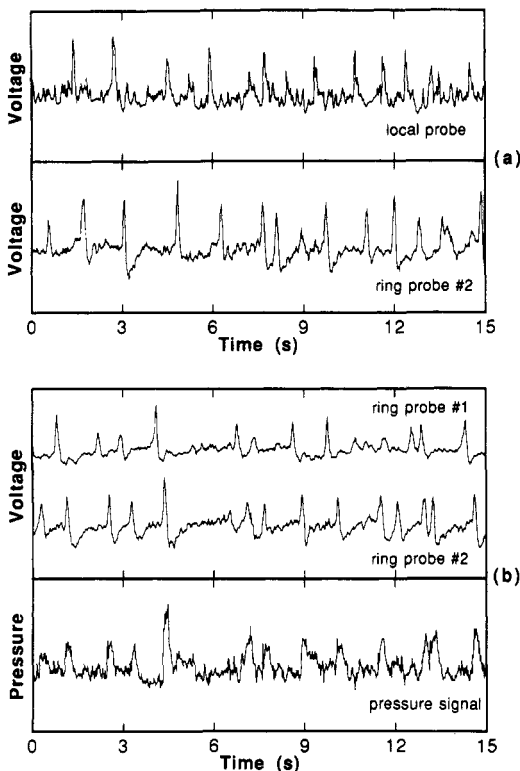


Figure 10. Comparison of simultaneously recorded traces from the conductance ring probes and from other techniques: (a) local probe and downstream ring probe; (b) ring probes and pressure transducer; $L = 10.85 \text{ kg/m}^2 \text{ s}$ and $G = 0.149 \text{ kg/m}^2 \text{ s}$.

the core of the bed are essentially the same as those in the entire cross section.

Recently, Tsochatzidis and Karabelas (1994) embedded microelectrodes on the surface of individual particles in the bed, to further explore conditions in the microscale. They did record instantaneous local mass transfer rates in pulsing flow, showing similarities (in the time macro-scale) with traces obtained from the conductance ring probes.

Figure 10b suggests that the ring probes are also superior, for detecting pulses, compared to a wall-mounted pressure transducer. The latter provides a local measurement with an influence from its vicinity, the spatial extent of which cannot be determined. In this case of wall pressure transducers one is concerned that even the dominant pulse frequency throughout the cross section may be misrepresented, in particular close to transition, where the pulse amplitude is small. For reasons outlined above the ring probes are preferred for determining the onset of pulsing.

Quantitative and Qualitative Information. To detect transition, the system was initially operated at high liquid rates in pulsing flow and then stabilized in the trickling flow regime. Tests for transition were made by keeping the liquid rate constant, while the gas flow rate was increased by small increments. It is significant to note that the first pulse was always clearly detected by the lower probe (mounted just above the column bottom) but it was *not visible* macroscopically.

Figure 11 shows a sequence of traces simultaneously recorded from the two conductance ring probes. The traces in Figure 11a correspond to trickling flow. Of special interest are the traces in Figure 11b, showing the formation of several gas-rich zones (marked with arrows) at the upstream probe, which evolve into distinct, liquid-rich, pulses downstream. The following parts c and d of Figure 11 provide evidence of the strong effect of gas velocity on

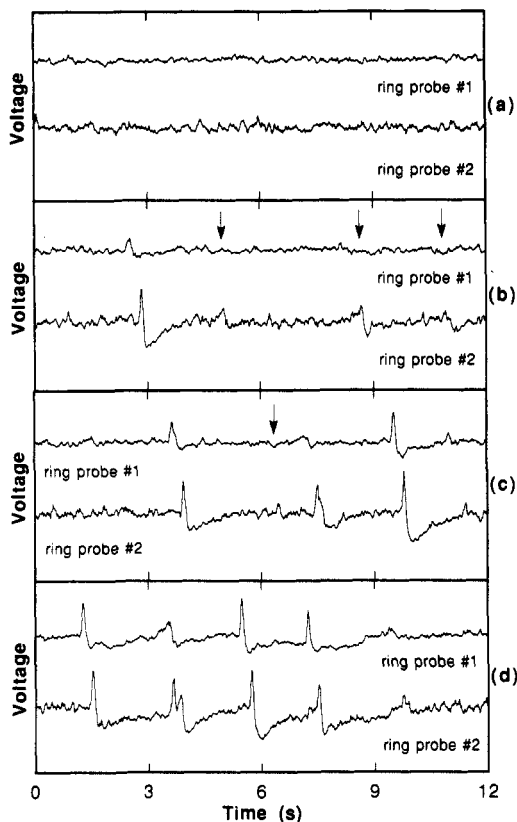


Figure 11. Traces from the ring probes at the transition boundary from trickling-to-pulsing flow. Constant liquid rate: $L = 8.921 \text{ kg/m}^2 \text{ s}$; (a) $G = 0.193$; (b) $G = 0.203$; (c) $G = 0.213$; (d) $G = 0.223 \text{ kg/m}^2 \text{ s}$.

pulsing flow development. Indeed, a slight increase of gas rate at the transition (Figure 11c) promotes a well-organized pulsing flow (Figure 11d). An intermediate gas flow rate between those of Figure 11b and c is considered to define the transition boundary.

Upon inspection of the above evidence one wonders about the origin of the first instrumentally detected but not visible pulses. For instance, it is not clear whether they are related to pulses not spanning the entire column cross section, as reported by Christensen et al. (1986) or to some liquid-rich clusters called "protopulses" by Melli et al. (1990). The latter observed protopulses originated in the upper part of the column and attributed their generation to the lower gas velocity there (than in the bottom section) and its inability to open up the passages. The pulse formation mechanism proposed by Melli et al. (1990), called "overtaking mechanism", is actually based on such liquid-rich clusters growing as they travel downward until they become noticeable (pulses) at the bottom of the bed.

The height of the test section (from the bottom) covered with pulses is a strong function of the flow rates. A small increase in the flow rates above the transition raises sharply the pulsing onset level in the column. Table 1 includes the bed height covered with pulses, as a function of the gas flow rate, obtained by macroscopic visual observations. The liquid flow rate is held constant. It is clear that a steep change in the pulse formation level is caused by a small increase of gas flow rate above the transition. Increasing the liquid flow rate, under constant gas flow rate, results in a similar and even more abrupt increase of the pulse formation level. The tests show that pulses are formed approximately 10 cm below the column entrance in fully developed pulsing flow (last line of the table).

Table 1. Height of the Bed, from the Bottom, Covered with Pulses, for Various Gas Flow Rates: $L = 10.85 \text{ kg/m}^2 \text{s}$

G ($\text{kg/m}^2 \text{s}$)	pulsing onset level (cm)	G ($\text{kg/m}^2 \text{s}$)	pulsing onset level (cm)
0.121	0 ^a	0.195	95–100
0.135	0 ^b	0.247	105–110
0.149	60–65	0.330	110–115
0.169	75–80		

^a Trickling flow. ^b Pulses not visible, transition detected only by conductance ring probes.

By reviewing all the evidence obtained in this study, one can stress the following observations: (i) Close to transition, extensive blockage of constricted passages is observed (Figure 7). (ii) Clearly detectable pulses (in the length and time macroscale) develop first at the bottom of the bed, where the gas velocity is comparatively higher (Figure 11b). (iii) Keeping the liquid flow rate constant, pulsing starts by slightly increasing the gas flow rate above a critical value (Figure 11). Additionally, attention is paid to the experimental results obtained by de Santos (1991) for flow through tubular constrictions, of diameter similar to the characteristic size of constricted passages in the present study. For annular film flow through such constrictions, de Santos (1991) observed a liquid film tendency to bulge just below the narrowest cross section. This is apparently a step before liquid bridging. All this evidence suggests that while the bed operates in the gas-continuous trickling, a very small increase of gas velocity leads to extensive blockage of constricted passages through a mechanism possibly related to the Bernoulli effect. Such occlusions may cause initially a relatively insignificant increase of liquid holdup but a rather sharp pressure buildup, with simultaneous gas accumulation in pores unable to discharge fluid through the blocked passages. The local pressure gradient thus developing may provide the necessary force to push liquid in the downstream direction, resulting in the formation of a moving liquid-rich zone. By comparing the peaks in signals from ring probe 2 and the neighboring pressure transducer (Figure 10b), one can detect a definite time lag between the holdup disturbance and the pressure wave. This time lag (documented in detail by Tsochatzidis, 1994) is evidence of the strong driving force moving liquid downward.

Comparisons with Previous Work. Several empirical flow regime maps have been developed by various researchers. These maps have been presented in terms of superficial mass flow rates of the phases, G vs L (e.g. Weekman and Myers, 1964; Sato et al., 1973; Satterfield, 1975). Charpentier and Favier (1975) have suggested a plot of $L\lambda\psi/G$ vs G/λ , in which λ and ψ depend on the physical gas and liquid properties. In the cases of air and water, $\lambda = \psi = 1$. Gianetto et al. (1978) have modified the abscissa using $G/\lambda\epsilon$, to take into account the effect of packing void fraction, and have compared the results of several studies in a flow map presented in Figure 12. Our data fall on a smooth line, which is in good agreement with most of these correlations, even though the scale of coordinates in Figure 12 does not permit a detailed comparison.

By interpretation of their data, Blok et al. (1983) observed that the transition, for each gas/liquid system and type of packing, occurred at almost the same real liquid velocity. On the basis of this observation, they developed an equation for the superficial liquid and gas velocities at transition. This correlation is in agreement with our data only at low gas velocities, deviating significantly with increasing gas velocity.

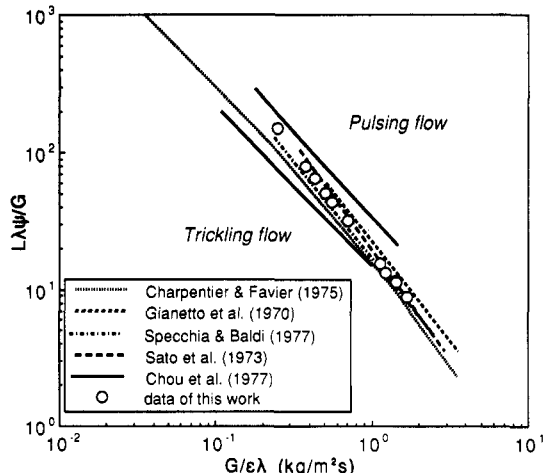


Figure 12. Trickling-to-pulsing flow regime transition (Gianetto et al., 1978). Comparison with present data.

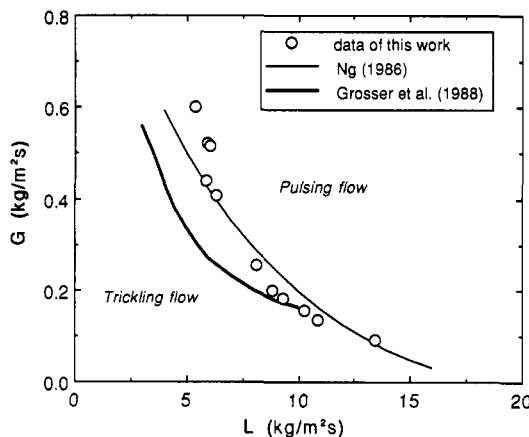


Figure 13. Comparison of theoretical models with experimental data for the transition boundary from trickling-to-pulsing flow.

Ng (1986) developed a model for predicting flow regime transition, based on physical arguments, motivated by similar approaches used in two-phase pipe flow. Applying Bernoulli's concept, this pore scale model takes into account all the significant system variables for nonfoaming liquids. In Figure 13 a comparison is made between the present data and Ng's model for transition from trickling to pulsing flow, showing an overall good agreement. The estimates of average liquid saturation required for the above comparison were obtained from a correlation suggested by Ng (1986).

Fair agreement is also observed between the present data and the theoretical macroscopic model of Grosser et al. (1988). Their model admits a uniform solution for given gas and liquid flow rates. The onset of pulsing is detected by applying one-dimensional perturbations and examining the linear stability of this uniform state. The line representing the Grosser et al. (1988) predictions in Figure 13 corresponds to their Model I. Results from another model proposed by Dankworth and Sundaresan (1992) overall are not in good agreement with the data, being close at the higher liquid flow rates, L , but deviating significantly with decreasing L .

Recently, Holub et al. (1993) adopted the loss of laminar film stability as a mechanism of transition from the low-to-high-interaction flow regime and developed a transition model based on Kapitza's criterion for the onset of interfacial waves on laminar liquid films. This criterion was applied to a pore-scale "slit" model and then mapped to the bed scale to predict trickling-to-pulsing transition.

The model is comprised of three inequalities and contains no empirical parameters except the Ergun constants that must be determined through single-phase flow experiments. From such experiments the Ergun equation coefficients for the present system are determined to be $E_1 = 195$ and $E_2 = 1.8$, which are very close to the universal Ergun constants reported in Holub et al. (1993) ($E_1 = 180$, $E_2 = 1.8$). Our data generally satisfy the inequalities of the model with the exception of few points at high liquid flow rates. For the latter conditions, however, the model does not seem to perform well (see also Figure 13 of Holub et al. (1993)).

Concluding Remarks

The visual study at a (length and time) microscale clearly shows the importance of constricted flow passages in the development of macroscopically observed flow regimes. The elemental patterns of gas/liquid flow through such constrictions, identified by Melli et al. (1990) in a two-dimensional test section, are also observed in the randomly packed bed of this work (with the possible exception of the spray pattern). In the case of relatively simple flow regimes such as the trickling, bubbling, and spray flow, the pores (or sites)—the other major component of the interstices—appear to be gas- or liquid-dominated or contested by both phases, depending on the flow rates. However, in the case of the incipient pulsing and developed pulsing flow regime, new evidence is presented concerning gas penetration into gas-dominated pores, through liquid-blocked passages. With surface tension forces apparently active, bubbles tend to form rapidly from the constrictions, covering the available pore space and vanishing over a time period on the order of 10 ms. This small time period may be attributed to the high real gas velocity (on the order of 1 m/s) and the small (a few millimeters) characteristic pore size. The significance of this gas penetration mechanism (for transport processes), yielding high gas/liquid interface renewal rates, cannot be overemphasized.

Close to onset of pulsing, occlusions of constricted passages appear to result in local pressure gradients, in the vertical direction, thus triggering liquid-rich zone formation. The cause of such occlusions is still unclear although there are indications of an instability, possibly induced by Bernoulli-type effects. A small flow rate increase (beyond the onset), leads to the well-organized pulsing regime. Total liquid blockage does not appear to occur throughout the bed cross section at any time. In fact there is a lot of evidence from the visual studies and from accurate holdup measurements (Tsoschatzidis, 1994) that the cross section never even comes close to the point of liquid saturation. These observations and the estimated length and time micro- and macroscales suggest that careful selection of experimental techniques should be made to correctly measure required average or local properties in trickle beds. For the purpose of diagnosing on-line the onset of pulsing flow, a conductance technique (Tsoschatzidis et al., 1992) is successfully employed and shown to be superior to other techniques reported in the literature. This technique allows one to make accurate instantaneous (cross sectionally averaged) holdup measurements and is currently used in a detailed study of pulsing flow characteristics.

Acknowledgment

The authors are grateful to the Commission of the European Communities for financial support of this work

under Contract JOU2-CT92-0067. Many thanks are due to Mr. V. Christoforou for his assistance in videotaping the flow.

Nomenclature

Bo	= Bond number, dimensionless
Ca	= capillary number, dimensionless
Re	= Reynolds number, dimensionless
D	= bed diameter, m
d_p	= particle diameter, m
G	= superficial mass flow rate of gas, kg/(m ² s)
g	= acceleration due to gravity, m/s ²
L	= superficial mass flow rate of liquid, kg/(m ² s)
R	= bed radius, m
r_p	= particle radius, m
U	= superficial velocity, m/s
u	= real velocity, m/s
ϵ	= bed porosity, m ³ void/m ³ column
μ	= dynamic viscosity, kg/(m s)
ρ	= density, kg/m ³
σ	= surface tension, N/m
λ	= flow parameter, dimensionless
ψ	= flow parameter, dimensionless

Subscripts

g	= gas phase
l	= liquid phase

Literature Cited

- Andreussi, P.; Di Donfrancesco, A.; Messia, M. An impedance method for the measurement of liquid hold-up in two phase flow. *Int. J. Multiphase Flow* 1988, 14, 777-785.
- Blok, J. R.; Drinkenburg, A. A. H. Hydrodynamic properties of pulses in two-phase downflow operated packed columns. *Chem. Eng. J.* 1982, 25, 89-99.
- Blok, J. R.; Varkevisser, J.; Drinkenburg, A. A. H. Transition to pulsing flow, holdup and pressure drop in packed columns with cocurrent gas-liquid downflow. *Chem. Eng. Sci.* 1983, 38, 687-699.
- Charpentier, J. C. Recent progress in two phase gas-liquid mass transfer in packed beds. *Chem. Eng. J.* 1976, 11, 161-181.
- Charpentier, J. C.; Favier, M. Some liquid holdup experimental data in trickle-bed reactors for foaming and nonfoaming hydrocarbons. *AIChE J.* 1975, 21, 1213-1218.
- Chou, T. S.; Worley, F. L., Jr.; Luss, D. Transition to pulsed flow in mixed-phase cocurrent downflow through a fixed bed. *Ind. Eng. Chem. Process Des. Dev.* 1977, 16, 424-427.
- Christensen, G.; McGovern, S. J.; Sundaresan, S. Cocurrent downflow of air and water in a two-dimensional packed column. *AIChE J.* 1986, 32, 1677-1689.
- Dankworth, D. C.; Sundaresan, S. Time-dependent vertical gas-liquid flow in packed beds. *Chem. Eng. Sci.* 1992, 47, 337-346.
- de Santos, J. M. Two-phase cocurrent downflow through constricted passages. Ph.D. Dissertation. University of Minnesota, Minneapolis, MN, 1991.
- de Santos, J. M.; Melli, T. R.; Scriven, L. E. Mechanics of gas-liquid flow in packed-bed contactors. *Annu. Rev. Fluid Mech.* 1991, 23, 233-261.
- Dudukovic, M. P.; Mills, P. L. Contacting and hydrodynamics in trickle-bed reactors. In *Encyclopedia of Fluid Mechanics*; Gulf Publishing Company: Houston, TX 1986; Vol. 3, pp 969-1017.
- Gianetto, A.; Specchia, V. Trickle-bed reactors: state of art and perspectives. *Chem. Eng. Sci.* 1992, 47, 3197-3213.
- Gianetto, A.; Baldi, G.; Specchia, V.; Sicardi, S. Hydrodynamics and solid-liquid contacting effectiveness in trickle-bed reactors. *AIChE J.* 1978, 24, 1087-1104.
- Grosser, K.; Carbonell, R. G.; Sundaresan, S. Onset of pulsing in two-phase cocurrent downflow through a packed bed. *AIChE J.* 1988, 34, 1850-1860.
- Helwic, J. A.; Dillon, P. O.; McCready, M. J. Time varying behavior of cocurrent gas-liquid flows in packed beds. *Chem. Eng. Sci.* 1992, 47, 3249-3256.
- Hershkowitz, M.; Smith, J. M. Trickle-bed reactors: A review. *AIChE J.* 1983, 29, 1-18.

- Hofmann, H. Hydrodynamics, transport phenomena, and mathematical models in trickle-bed reactors. *Int. Chem. Eng.* 1977, 17, 19-28.
- Holub, R. A.; Dudukovic, M. P.; Ramachandran, P. A. Pressure drop, liquid holdup, and flow regime transition in trickle flow. *AICHE J.* 1993, 39, 302-321.
- Kolb, W. B.; Melli, T. R.; de Santos, J. M.; Scriven, L. E. Cocurrent downflow in packed beds. Flow regimes and their acoustic signatures. *Ind. Eng. Chem. Res.* 1990, 29, 2380-2389.
- Latifi, M. A.; Rode, S.; Midoux, N.; Storck, A. The use of micro-electrodes for the determination of flow regimes in a trickle-bed reactor. *Chem. Eng. Sci.* 1992, 47, 1955-1961.
- Lutran, P. G.; Ng, K. M.; Delikat, E. P. Liquid distribution in trickle beds. An experimental study using computer-assisted tomography. *Ind. Eng. Chem. Res.* 1991, 30, 1270-1280.
- Melli, T. R.; de Santos, J. M.; Kolb, W. B.; Scriven, L. E. Cocurrent downflow in networks of passages. Microscale roots of macroscale flow regimes. *Ind. Eng. Chem. Res.* 1990, 29, 2367-2379.
- Ng, K. M. A model for flow regime transitions in cocurrent downflow trickle-bed reactor. *AICHE J.* 1986, 32, 115-122.
- Saez, A. E.; Carbonell, R. G. Hydrodynamic parameters for gas-liquid cocurrent flow in packed beds. *AICHE J.* 1985, 31, 52-62.
- Sato, Y.; Hirose, T.; Takahashi, F.; Toda, M.; Hashiguchi, Y. Flow Pattern and Pulsation Properties of Cocurrent Gas-Liquid Downflow in Packed Beds. *J. Chem. Eng. Jpn.* 1973, 6, 315-319.
- Satterfield, C. N. Trickle-bed reactors. *AICHE J.* 1975, 21, 209-228.
- Sicardi, S.; Gerhard, H.; Hofmann, H. Flow regime transition in trickle bed reactors. *Chem. Eng. J.* 1979, 18, 173-182.
- Tsochatzidis, N. A. A study of two-phase cocurrent downflow in packed beds: Pulsing flow. Ph.D. Dissertation, Aristotle University of Thessaloniki, Greece, 1994.
- Tsochatzidis, N. A.; Karabelas, A. J. Hydrodynamic properties of pulses in trickle beds. In *Proceedings of the 2nd World Conference on Experimental Heat Transfer, Fluid Mechanics and Thermodynamics*; Keffer, J. F., Shah, R. K., Ganic, E. N., Eds.; Elsevier: Amsterdam, The Netherlands, 1991; pp 1515-1522.
- Tsochatzidis, N. A.; Karabelas, A. J. Study of pulsing flow in a trickle bed using the electrodiffusion technique. *J. Appl. Electrochem.* 1994, in press.
- Tsochatzidis, N. A.; Karapantsios, T. D.; Kostoglou, M. V.; Karabelas, A. J. A conductance probe for measuring liquid fraction in pipes and packed beds. *Int. J. Multiphase Flow*, 1992, 18, 653-667.
- Weekman, V. W., Jr.; Wyers, J. E. Fluid-flow characteristics of cocurrent gas-liquid flow in packed beds. *AICHE J.* 1964, 10, 951-957.

Received for review August 18, 1993

Revised manuscript received January 24, 1994

Accepted January 31, 1994*

* Abstract published in *Advance ACS Abstracts*, March 15, 1994.